The Aza-Payne Rearrangement: A Theoretical DFT Study of the Counter-Ion and Solvent Effects

Abdelatif Bouyacoub[a,b] and François Volatron*[a]

Keywords: Aza-Payne rearrangement / B3LYP calculations / Nucleophilic substitution / Reaction mechanisms / Solvent effects

The aza-Payne reaction mechanism has been studied by theoretical DFT calculations. Three reaction pathways have been considered: two of them result in the formation of a three-membered ring, with either inversion (S_NI, experimentally observed) or retention (S_NR) at the substituted carbon. The third reaction path results in the formation of a four-membered ring. The mechanisms were first studied in the gas phase with the bare anion (An^-). The role of the counter-ion (Li^+) was then analysed by study of the reaction with the neutral species ($An^- Li^+$) in the gas phase. Results for the ($An^- Na^+$) system are also presented. Finally, the role of the solvent (THF and H_2O) was taken into account with the aid of a cavity model. We found that the S_NI mechanism was most favoured in anionic gas phase and for the neutral species in solution. Surprisingly, the S_NR mechanism was found to be the most favourable one in the gas phase for neutral species in both cases (Li^+ and Na^+). These findings are interpreted by consideration of the interactions that may develop between the anion and the counter-ion in transition states and are discussed in the light of experimental data on these systems.

Introduction

The Payne reaction[1] is an epoxide migration that generally occurs under basic conditions (Scheme 1). Its mechanism is intramolecular S_N2, proceeding through an inversion of configuration at the C_2 carbon.

Scheme 1

This anionic reaction has also been studied in combined experimental (gas phase) and theoretical studies.[2−4] A similar reaction may occur under basic conditions with epoxy-amine reactants (aza-Payne reaction, Scheme 2).[5−7]

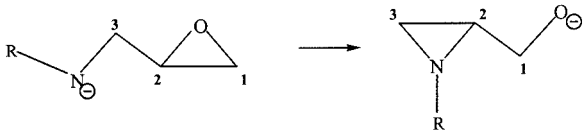

Scheme 2

In this case, epoxide opening is achieved through nucleophilic attack at the C_2 carbon. As in the Payne reaction, the aza-Payne reaction proceeds with inversion of configuration at the C_2 carbon, which indicates an S_N2 mechanism. Under basic conditions, the reaction yield strongly depends on the natures of the solvent and of the counter-ion. In the case of primary amines, the use of *n*BuLi for anion formation in THF gives reasonable yields only when a Lewis acid ($AlMe_3$) is added.[5] Higher yields are obtained when the "super-base" *n*BuLi/*t*BuOK is used in a mixed *n*-hexane/THF solvent.[6] In this latter case, no Lewis acid is needed for obtaining yields close to 80%. [An exception is, however, found when the C_2 carbon is substituted with a methyl group; steric effects may be then responsible for the low (40%) yield.] The reaction becomes easier when a tosyl group is substituted at the nitrogen atom. A 81−93% conversion ratio is obtained under "Payne conditions" (aqueous sodium hydroxide solution).[7] A detailed study of the aza-Payne rearrangement of such *n*-tosyl-substituted epoxy-

[a] Laboratoire de Chimie Physique (UMR 8000), Bât. 490, Université de Paris-Sud,
91405, Orsay Cedex, France
Fax: (internat.) +33−1/69 15 44 47
E-mail: volatron@lcp.u-psud.fr
[b] Laboratoire de Chimie Physique Macromoléculaire, Département de Chimie; Faculté des Sciences, Université d'Oran Es-Sénia,
Oran, Algérie
E-mail: latif@lcp.u-psud.fr

amines under various conditions[6] suggested the following conclusions:

(i) Bases such as *n*BuLi or LDA in THF do not give efficient rearrangement. In contrast, NaH, KH, or *t*BuOK give satisfactory results.

(ii) THF or mixed THF/HMPA is a solvent of choice.

(iii) Rearrangement yields strongly depend on temperature.

Aza-Payne rearrangement under basic[8] or neutral[9] conditions has been reviewed recently.

To the best of our knowledge, only one theoretical study[6] on the aza-Payne reaction has been published. However, since this study deals with aziridines substituted with SO_2Me groups, these results are not directly comparable to ours.

The aim of this paper is to study the anionic aza-Payne rearrangement by theoretical means in order to investigate the reaction mechanism and the role of the reaction conditions. The gas-phase anionic reaction is studied first. The influence of the counter-ion (restricted to the Li^+ and Na^+ cations) is then taken into account. Finally, the potential energy surface associated with the neutral anion/counter-ion system is recalculated with the aid of a continuum model that simulates the role of the solvent.

Method of Calculation

The Gaussian set of programs was used throughout.[10] Since anionic species are involved in the various reactions under study, the 6-31+G* basis set containing diffuse functions was chosen.[11] All the extrema were optimized and characterized at the DFT/B3LYP level.[12] Frequencies calculations indicated the natures of the extrema: a minimum and a transition state (TS) are characterized by zero and only one imaginary frequency, respectively. Solvation effects were taken into account by use of the Onsager cavity model, which creates an electric field inside a cavity which contains the solute.[13] This model gives a reasonable description of the solvent effect as long as no important role is played by solvent molecules in the first solvation sphere. All the extrema (minima and transition states) were reoptimized and characterized within this formalism. Optimized geometries and absolute energies are available upon request.

Results

Three pathways were envisaged. In the first, which corresponds to the classical S_N2 pathway, the anionic nitrogen atom attacks the substituted carbon C_2 on the epoxide, with inversion of configuration at this carbon. The second reaction pathway still involves attack by the amino group at the substituted epoxide carbon C_2, but with retention of the carbon configuration (i.e., the nitrogen atom is located on the same side as the oxygen atom in the transition state). Finally, attack at the epoxide unsubstituted carbon C_1, giving a four-membered ring azetidine, is also considered.

A Gas-Phase Anionic Pathways

1) Reactants

The anionic substituted oxirane was fully optimized. Seven minima were found on the potential energy surface (PES) and are depicted in Figure 1. They may easily be classified by noting that, basically, two degrees of freedom may be considered: rotations about the CC bond (θ) and about the CN bond (φ) (Scheme 3).

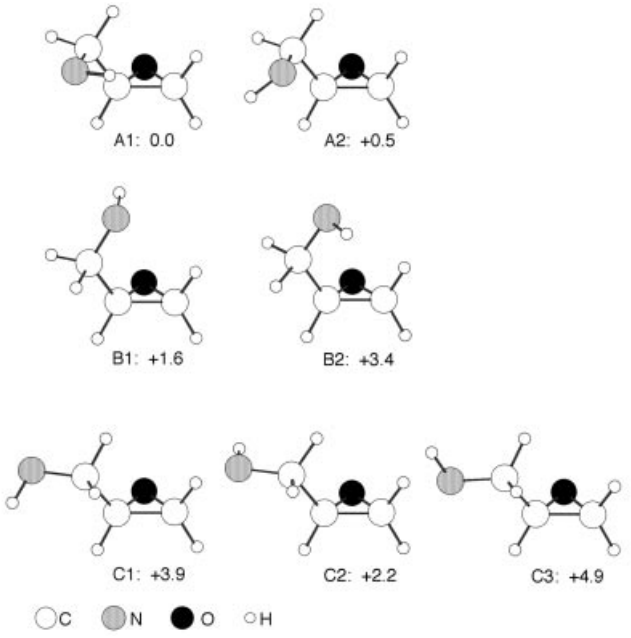

Figure 1. Structure and relative energies (in kcal/mol) of the conformers of the anionic reactant

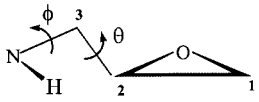

Scheme 3

For each minimum, the optimal values of two parameters (θ and φ) roughly correspond to a staggered conformation about the CC and CN bond. Among the seven conformers, those with N and O atoms in antiperiplanar orientations (structures **A1** and **A2**) were found to be the most stable: this stability comes from the interaction of the nitrogen lone pair with the antibonding σ^*_{CO} orbital. A similar interaction has been found to be behind the anomeric effect.[14] On the whole, the energy differences between the various conformers are small (less than 5 kcal/mol).

2) Products

Two series of products were calculated and the results are given in Figure 2. The first series (**P31s−P33a**) corresponds to a substituted aziridine, which is the experimentally ob-

served product. Two invertomers [*syn* (**s**) or *anti* (**a**)] were found, depending on the relative positions of the exocyclic carbon atom and hydrogen atom bound to the nitrogen (H_N). For each invertomer, rotation about the CC bond produces three different conformers. As in the reactants, the optimal values of this rotation angle roughly correspond to staggered conformations of the product (relative to the CC bond).

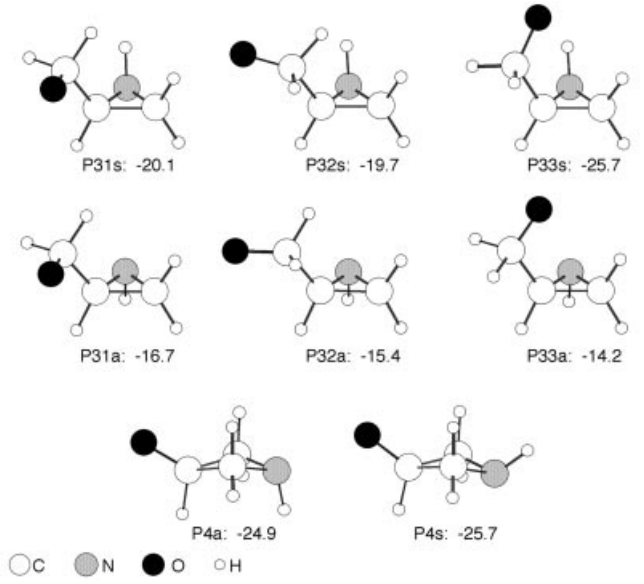

Figure 2. Structure and relative energies (in kcal/mol) of the isomers of the anionic products

The lowest-energy structure of the substituted aziridine (**P33s**, $\Delta E = -25.7$ kcal/mol) is found for a *cis* arrangement of the N and O atoms. This high stability may arise from the formation of a hydrogen bond between O and H_N atoms. On the whole, the *syn* invertomers were found to be more stable ($\Delta E = -19.7/-25.7$ kcal/mol) than the *anti* invertomers ($\Delta E = -14.2/-16.7$ kcal/mol). The second calculated product was the azetidine resulting from the formation of a N−C bond at the unsubstituted carbon atom. As in the preceding case, *syn* and *anti* invertomers were obtained. Only two minima [one *syn* (**P4s**) and one *anti* (**P4a**)] were located on the PES. The *syn* isomer was found to be slightly more stable ($\Delta E = -25.7$ kcal/mol) than the *anti* isomer ($\Delta E = -24.9$ kcal/mol).

3) Transition States

As described in the Introduction, three different pathways were envisaged: two S_N2 mechanisms − with either carbon configuration inversion (S_NI) or retention (S_NR) − resulting in the formation of a three-membered cycle, and formation of a four-membered cycle (S_N4). In this latter case, only the inversion pathway may be envisaged, for obvious geometrical reasons. The results are summarized in Figure 3 and Table 1.

In the S_NI pathway, two transition states were characterized (**TSIs** and **TSIa**). These give rise to *syn* or *anti* products depending on the relative positions of the O and H_N atoms, as discussed above. Both transition states were found to be

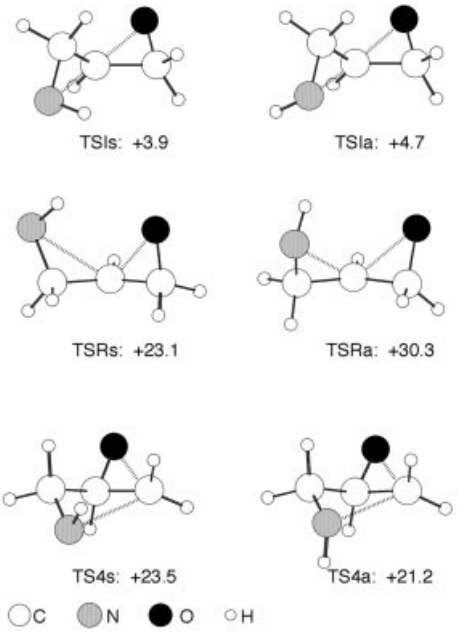

Figure 3. Structures and relative energies (in kcal/mol) of the anionic transition states

Table 1. Relative energies (in kcal/mol) and main geometrical parameters (in Å and degrees) of the anionic transition states

	s	a	
ΔE	**3.9**	**4.7**	
NC	2.213	2.204	**TSI**
CO	1.821	1.829	
NCO	157.6	157.2	
ΔE	**23.1**	**30.3**	
NC	2.298	2.330	**TSR**
CO	2.080	2.047	
NCO	91.1	90.9	
ΔE	**23.5**	**21.2**	
NC	2.556	1.525	**TS4**
CO	1.975	1.962	
NCO	106.3	107.7	

low in energy, which reflects the strong nucleophilicity of the bare anionic (NH^-) group. The *syn* transition state (**TSIs**) is slightly lower in energy ($\Delta E = +3.9$ kcal/mol) than the *anti* transition state (**TSIa**, $\Delta E = +4.7$ kcal/mol), in accordance with Hammond's postulate. In both cases, the N−C−O angle is large [N−C−O = 157.6° (**TSIs**) and 157.2° (**TSIa**)], showing, as expected, a quasi-bipyramidal coordination of the carbon atom in the transition state.

Two transition states [*syn* (**TS4s**) and *anti* (**TS4a**)] were characterized for the formation of a four-membered ring (Table 1 and Figure 3). Their energies ($\Delta E = +23.5$ and 21.2 kcal/mol, respectively) were substantially higher than the values obtained for the S_NI inversion pathway. Similar results have been obtained in theoretical study of the Payne reaction.[3]

Finally, the pathway with retention of configuration (S_NR) also resulted in the characterization of two transition states (**TSRs** and **TSRa**), both high in energy (ΔE = +23.1 and + 30.3 kcal/mol respectively).

In conclusion of this anionic gas-phase pathway study, the following points should be emphasized:

(i) The S_NI pathway is clearly kinetically favoured over the two other mechanisms.

(ii) In the S_NI pathway, production of the *syn* isomer is preferred on both thermodynamic and kinetic grounds.

(iii) The computed activation energy (3.9 kcal/mol) is small, in accordance with the high nucleophilicity of a bare anionic (NH^-) group.

B Neutral Species Pathways

In order to obtain a more accurate description of the reaction pathways, the different extrema (reactants, products and transition states) were reoptimized, taking the counter-ion [M^+] into account in each case. Two cases for which experimental data are available ($M^+ = Li^+$ and Na^+) were considered. First we discuss the PES associated with the Li^+ cation.

1) Reactants

Seven minima were found for the reactant in complexation with a lithium cation; the results are shown in Figure 4. As in the anionic species, these structures may be classified with respect to the dihedral angles NCCO and HNCC. The three **A** conformers in which N is antiperiplanar to O are close in energy (ΔE = 13.7−14.7 kcal/mol) and are no longer the most stable ones on the PES.

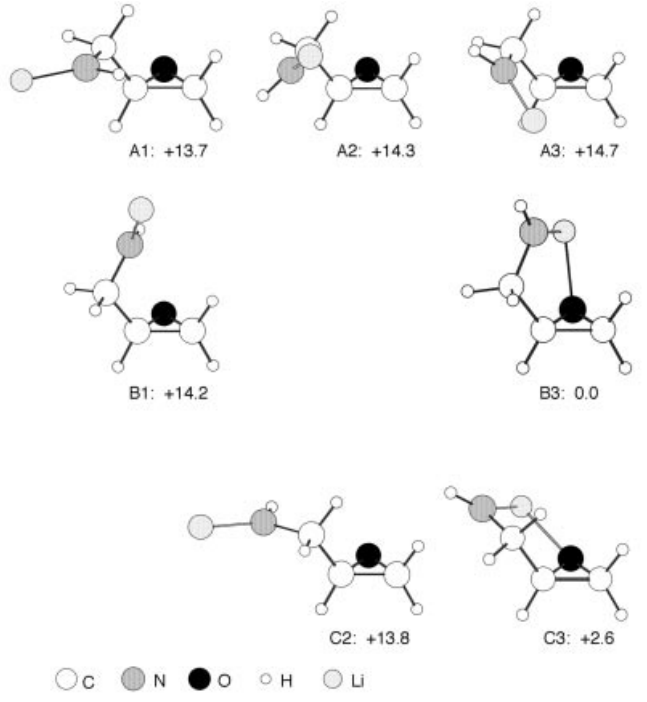

Figure 4. Structures and relative energies (in kcal/mol) of the conformers of the neutral reactant

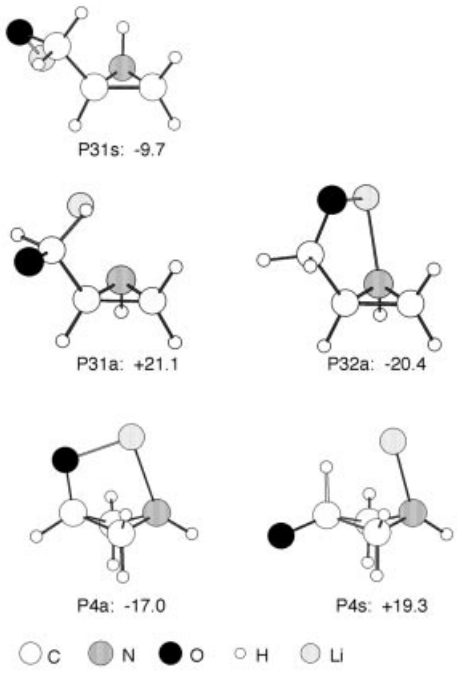

Figure 5. Structures and relative energies (in kcal/mol) of the isomers of the neutral products

We found the **B3** structure to be the lowest in energy. Its large stability is attributable to the simultaneous coordination of the Li^+ cation both to oxygen and to nitrogen (Li−O = 1.924 Å; Li−N = 1.794 Å). In fact (see below), the possibility of chelation of both electronegative atoms by the Li^+ cation is the prominent feature in this series of neutral compounds. In **C3**, this chelation may occur and this conformer is slightly above (2.6 kcal/mol) the minimum **B3**. The **B1** isomer, in which such chelation is not possible, was found to be 14.2 kcal/mol higher in energy than the preceding absolute minimum, a value close to those found for the three **A** isomers.

2) Products

In both products (three- or four-membered rings), the anionic site is localized on the oxygen atom. Consequently, complexation by the Li^+ cation should occur preferentially on this atom rather than on the neutral nitrogen atom. However, since Li^+ is bound to nitrogen in the reactants, the complexation site change demands a Li^+ transfer from N^- to O. This migration is possible, without being energetically prohibitive, only through chelated structures in which both atoms interact with the Li^+ cation. Such chelated structures were found to be the most stable in the reactant case. Consequently, for the products, we only optimized chelated and Li^+−N bonded structures.

For the three-membered ring products, only three minima were located (one *syn* and two *anti*, Figure 5). The most stable one (**P32a**, ΔE = −20.4 kcal/mol with respect to the most stable reactant) was found in the *anti* conformation of the aziridine. Again, this large stability is attributable to the chelation of nitrogen and oxygen by lithium (Li−O = 1.719 Å; Li−N = 1.990 Å) as discussed above.

Two four-membered ring products were located on the PES (Figure 5). In the most stable one (**P4a**), chelation between the N and O atoms was observed ($\Delta E = -17.0$ kcal/mol). The second isomer was energetically disfavoured since it has only one Li···N bond (**P4s**, $\Delta E = +19.3$ kcal/mol).

3) Transition States

As in the anionic study, six transition states were located. Their geometries and main structural characteristics are shown in Figure 6 and Table 2.

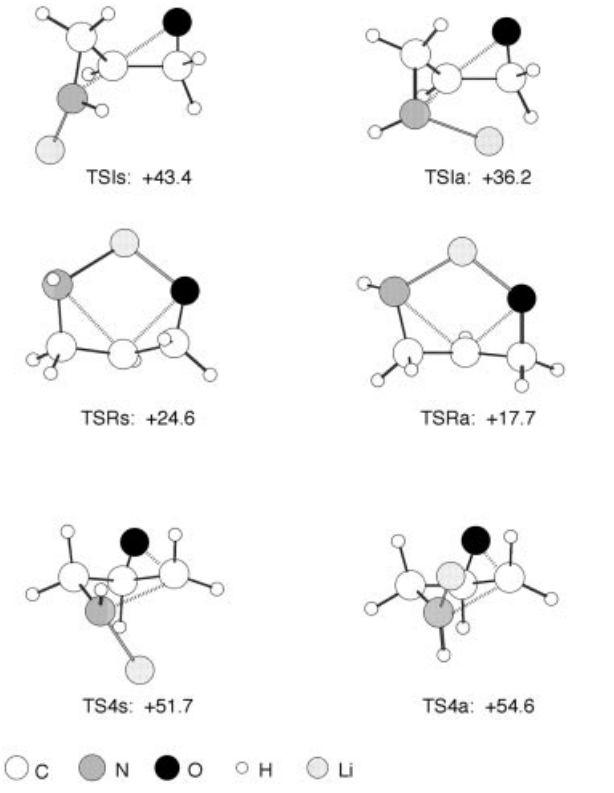

Figure 6. Structures and relative energies (in kcal/mol) of the transition states of the neutral species

Table 2. Relative energies (in kcal/mol) and main geometrical parameters (in Å and degrees) of the neutral transition states

	s	**a**	
ΔE	**43.4**	**36.2**	
NC	1.833	1.996	**TSILi**
CO	2.109	1.981	
ΔE	**24.6**	**17.7**	
NC	2.310	2.267	**TSRLi**
CO	2.067	2.065	
ΔE	**51.7**	**54.6**	
NC	2.316	2.185	**TS4Li**
CO	2.136	2.129	

a) S_NI pathways: two transition states (**TSILia** and **TSILis**) were characterized, giving rise to *anti* ($\Delta E = +36.2$ kcal/mol) and *syn* ($\Delta E = +43.4$ kcal/mol) products, respectively. These high activation energies are the result of the deactivation (relative to the anionic case) of the nitrogen lone pair by Li^+ complexation. In addition, since N and O atoms are in a roughly linear arrangement, no Li^+ chelation of these two atoms is geometrically possible in either S_NI transition state. As a consequence, these structures are high in energy.

b) Four-membered ring formation: two transition states were also characterized for this reaction pathway. They give *syn* (**TS4Lis**) and *anti* (**TS4Lia**) products and are high in energy ($\Delta E = +51.7$ and $+54.6$ kcal/mol respectively). Again, these high energies (relative to the anionic case) reflect nitrogen lone pair deactivation by Li^+ cation.

c) S_NR pathways: two transition states were characterized on the PES, corresponding to the formation of *anti* (**TSRa**) and *syn* (**TSRs**) three-membered rings, respectively. Chelation of N and O atoms by lithium cation occurs in both of them, and, consequently, both were found to be much lower in energy ($\Delta E = +17.7$ and $+24.6$ kcal/mol, respectively) than the preceding transition states. As a result, this pathway is the most favourable one.

In conclusion of this neutral pathway study, the following points should be noted:

(i) When Li^+ cation is present, chelated structures are strongly favoured over non-chelated ones. This feature is verified in the structures of the reactants, products and transition states.

(ii) Dramatic changes occur in the relative energies of the TSs. When Li^+ cation is present, the S_NR mechanism, in which retention of configuration at carbon occurs, becomes the most favoured pathway, a surprising result originating from the possibility of Li^+ chelation in the transition state.

4) Na^+ Cation Results

The energetic results obtained when a sodium cation was used instead of a lithium cation are given in Table 3−5, together with those obtained previously (Li^+ case) for purposes of comparison. The two sets of results are very similar: for the reactant, the most stable conformers were found when Na^+ chelation occurs between N and O (minimum **B3**, Table 3). The non-chelated minima are located 9−11 kcal/mol above the absolute minimum.

Table 3. Relative energies (in kcal/mol) of the neutral reactant (Na^+ as counter-ion). The results for Li^+ are also given for purposes of comparison

M	Li			Na			
	1	2	3	1	2	3	
ΔE	**13.7**	**14.3**	**14.7**	**9.8**	**10.5**	**10.9**	**A**
ΔE	**14.2**		**0.0**	**10.6**		**0.0**	**B**
ΔE		**13.8**	**2.6**		**10.2**	**0.8**	**C**

Table 4 gives the results for the products in the Li^+ and Na^+ cases. Again, the two sets of results are very similar.

The energetic ordering of the transition states was the same as found in the Li^+ case (Table 5): again, the S_NR

Table 4. Relative energies (in kcal/mol) of the neutral products (Na^+ as counter-ion). The results for Li^+ are also given for purposes of comparison

M	Li		Na	
	P31s	–	**P31s**	–
ΔE	**−9.7**		−13.3	
	P31a	**P32a**	**P31a**	**P32a**
ΔE	21.1	−20.4	12.5	−19.5
	P4a	**P4s**	**P4a**	**P4s**
ΔE	−17.0	19.3	−19.0	9.2

Table 5. Relative energies (in kcal/mol) and main geometrical parameters (in Å and degrees) of the neutral transition states (Na^+ as counter-ion). The results for Li^+ are also given for purposes of comparison

M	Li		Na		
	s	**a**	**s**	**a**	
ΔE	**43.4**	**36.2**	**34.5**	**28.2**	
NC	1.833	1.996	1.903	2.031	**TSI**
CO	2.109	1.981	2.079	1.972	
ΔE	**24.6**	**17.7**	**25.6**	**19.0**	
NC	2.310	2.267	2.347	2.270	**TSR**
CO	2.067	2.065	2.039	2.107	
ΔE	**51.7**	**54.6**	**44.7**	**47.4**	
NC	2.316	2.185	2.363	2.220	**TS4**
CO	2.136	2.129	2.112	2.091	

pathway was the most favourable one because of chelation by the cation in the transition state. Both S_NI and S_N4 transition states are energetically disfavoured (ΔE = +28.2 and +44.7 kcal/mol respectively).

C Solvent Effects

All the extrema found in the neutral cases ($M^+ = Li^+$ or Na^+) were reoptimized with solvent effects taken into account (THF and water). On the whole, these extrema were found to be closely analogous to those described in the preceding section: geometrical changes were minor and the main differences were energetic in nature.

1) Reactants

Optimized relative energies for reactants complexed by Li^+ and Na^+ in THF and water are given in Table 6. Gas-phase results are also reported for purposes of comparison.

For the reactants, it can be seen that the main trends observed in the gas phase remain valid in solution: the two chelated structures (**B3** and **C3**) were found to be the most stable in comparison to the non-chelated structures (Table 6). In the Li^+ case, the **B3** structure is the absolute minimum both in THF and in water as solvents. However, the energy differences between the chelated and non-chelated structures decrease from the gas phase (14.7 kcal/mol) to THF (11.9 kcal/mol) and to water (11.1 kcal/mol). This

Table 6. Relative energies (in kcal/mol) of the neutral reactants in the gas phase, in THF and in water

	Li^+			Na^+		
	Gas	THF	Water	Gas	THF	Water
A1	13.7	9.3	8.2	9.8	2.1	0.0
A2	14.3	7.3	5.3	10.5	4.0	2.4
A3	14.7	11.9	11.1	10.9	–	–
B1	14.2	7.1	5.1	10.5	5.6	4.5
B3	0.0	0.0	0.0	0.0	0.0	0.1
C2	13.8	9.4	8.1	10.2	4.1	2.5
C3	2.6	1.7	1.3	0.8	0.9	0.8

result may easily be explained, since solvent effects are expected to stabilize polar structures: the larger the dipole moment, the greater the stabilization. Consequently, chelated structures in which the Li^+ cation is close to the oxygen atom should be little stabilized by the solvent since their dipole moments are small. In contrast, non-chelated structures in which the Li^+ cation is remote from the oxygen atom should be more stabilized. Since chelated structures were found to be the most stable in the gas phase, the relative energies of the chelated and the non-chelated structures are smaller in solvent than in the gas phase. In addition, when the relative permittivity of the solvent increases from THF (ε = 7.6) to water (ε = 80.1) solvent effects become larger, which reduces the energy differences between the various conformations of the reactants.

Similar trends were found in the Na^+ cation case (Table 6). The energy differences decrease with increasing solvent stabilization, from 10.9 kcal/mol (gas phase) to 5.6 kcal/mol (THF) and 4.5 kcal/mol (water). Note that the solvent effect in water is large enough to give a non-chelated structure (**A1**) as the absolute minimum.

2) Products

The energetic results are summarized in Table 7. For the sake of simplicity, only the most stable conformers are given. Almost no influence of the solvent can be found in the relative energies of the products (Table 7), contrarily to what is observed with the reactants. This is a result of the fact that the cation (Li^+ or Na^+) chelates the two electronegative atoms in all the most stable products' geometries. As a consequence, no dramatic change, as was the case among the reactants, is observed.

3) Transition States

Energetic results for the gas-phase and solvated transition states are given in Table 8.

The energetic evolution of the transition states when solvent effects are taken into account is very similar to that discussed in the case of the reactants. Chelated structure energies are almost unchanged, whereas non-chelated structures are strongly stabilized. S_NR pathways with lithium cation, for instance, are practically insensitive to the presence of the solvent (ΔE = 24.6−25.6 kcal/mol for *syn* TS and 17.7−18.3 kcal/mol for *anti* TS). Results are different

Table 7. Relative energies (in kcal/mol) of the neutral products in the gas phase, in THF and in water

		P3s	P3a	P4a
	Gas	−9.7	−20.4	−17.0
Li	THF	−11.3	−23.6	−18.9
	Water	−11.7	−24.4	−19.3
	Gas	−13.3	−19.5	−19.0
Na	THF	−15.0	−24.0	−20.8
	Water	−15.3	−25.0	−21.0

Table 8. Relative energies (in kcal/mol) of the neutral transition states in the gas phase, in THF and in water

		TSIs	TSIa	TSRs	TSRa	TS4s	TS4a
Li	Gas	43.4	36.2	24.6	17.7	51.7	54.6
	THF	21.0	18.2	25.4	18.2	37.9	41.7
	Water	15.8	14.4	25.6	18.3	33.0	38.3
Na	Gas	34.5	28.2	25.6	19.0	44.7	47.4
	THF	17.6	12.9	27.0	20.8	26.6	24.4
	Water	13.8	7.7	27.4	21.4	20.2	18.0

for the TSs resulting in formation of the four-membered ring. Since the TSs are non-chelated in this case, their relative energies are lowered by the solvent effect: from 51.7 to 33.0 kcal/mol (Li^+) and from 44.7 to 20.2 kcal/mol (Na^+) for *syn* TS. The same trends hold for the S_NI inversion pathway. Moreover, since M^+ cation and oxygen atom are remote from each other in the transition state geometry, the degrees of stabilization of these TSs are fairly large: from 36.2 to 14.4 kcal/mol (Li^+ case) and from 28.2 to 7.7 kcal/mol (Na^+ case) for the *anti* TS, with similar trends being found for the *syn* TS.

As a result, the preferred mechanism drastically changes between the neutral gas-phase reactants and the solvated species. Whatever the nature of the cation, the S_NR pathway is the most favoured mechanism in the gas phase (and affords the *anti* isomer) whereas the S_NI mechanism becomes most favourable when solvent effects are taken into account.

4) Comparison with Experimental Data

The lowest-energy pathways, depending on the natures of the counter-ion and the solvent, are brought together in Table 9.

Table 9. Most favourable pathways, depending on the natures of the counter-ion and the solvent. The activation energies (in kcal/mol) are given in parentheses

	Gas	THF	Water
Anionic	S_NI (3.9)	−	−
Li^+	S_NR (17.7)	$S_NI = S_NR$ (18.2)	S_NI (14.4)
Na^+	S_NR (19.0)	S_NI (12.9)	S_NI (7.7)

The inversion pathway (S_NI) is preferred in almost all the cases, except for that of the neutral species in the gas phase.

The aza-Payne reaction has been shown to be easy in water as solvent with Na^+ as cation, a case in which our theoretical activation energy was found to be equal to 7.7 kcal/mol, the lowest value found from our theoretical calculations. When the cation is Li^+, the reaction in THF requires a 18.2 kcal/mol activation energy, a value substantially higher than that found in the preceding case. This findings agree with the experimental data: this reaction does occur but, unlike in the (Na^+/water) case, the presence of a catalyst ($AlMe_3$) is needed. Finally, it can be predicted from our results that this reaction should be possible in the presence of Na^+ in THF (ΔE = 12.9 kcal/mol), although it would be less easy than in water (ΔE = 7.7 kcal/mol).

Conclusion

Our theoretical study of the aza-Payne reaction shows this reaction to be sensitive both to the nature of solvent and to the presence of the counter-ion, these two effects acting in opposite senses. In the gas phase we found that the S_N2 mechanism was preferred. Neutral species should preferentially react through a S_NR mechanism, whatever the nature of the cation ($M^+ = Li^+$ or Na^+). Finally, solvent effects stabilize TSs with large dipole moments and, as a consequence, favour the S_N2 mechanism, as observed experimentally. Finally, we want to emphasize that our theoretical values should be only an estimate of the actual values because the correlation energy is only partly taken into account at our level of calculation (DFT/B3LYP). In addition, neither substituent effects, nor the first solvation shell of the cation have been taken into account in the model we have chosen. However, the evolution of the activation energies we have found from anionic gas phase to neutral species and to solvated species should be realistic.

[1] G. B. Payne, *J. Org. Chem.* **1962**, *27*, 3819−3822.
[2] S. Dua, M. S. Taylor, M. A. Buntine, J. H. Bowie, *J. Chem. Soc., Perkin Trans. 2* **1997**, 1991−1997.
[3] S. Dua, J. H. Bowie, M. S. Taylor, M. A. Buntine, *Int. J. Mass Spectrom. Ion Processes* **1997**, *165*, 139−153.
[4] J. M. Hevko, S. Dua, M. S. Taylor, J. H. Bowie, *Int. J. Mass Spectrometry* **1999**, *185*, 327−341.
[5] R. Najime, S. Pilard, M. Vaultier, *Tetrahedron Lett.* **1992**, *33*, 5351−5354.
[6] T. Ibuka, K. Nakai, H. Habashita, Y. Hotta, A. Otaka, N. Mimura, Y. Miwa, T. Taga, Y. Chounan, Y. Tamamoto, *J. Org. Chem.* **1995**, *60*, 2044−2058.
[7] J. Moulines, P. Charpentier, J.-P. Bats, A. Nuhrich, A.-M. Lamidey, *Tetrahedron Lett.* **1992**, *33*, 487−490.
[8] T. Ibuka, *Chem. Soc. Rev.* **1998**, *27*, 145−154.
[9] C. M. Rayner, *Synlett* **1997**, 11−21.
[10] *Gaussian 98*, Revision A. 1, M. J. Frisch, G. W. Trucks, H. B. Schlegel, G. E. Scuseria, M. A. Robb, J. R. Cheeseman, V. G. Zakrzewski, J. A. Montgomery, R. E. Stratmann, J. C. Burant, S. Dapprich, J. M. Millam, A. D. Daniels, K. N. Kudin, M. C. Strain, O. Farkas, J. Tomasi, V. Barone, M. Cossi, R. Cammi, B. Mennucci, C. Pomelli, C. Adamo, S. Clifford, J. Ochterski, G. A. Petersson, P. Y. Ayala, Q. Cui, K. Morokuma, D. K. Malick, A. D. Rabuck, K. Raghavachari, J. B. Foresman, J.

Cioslowski, J. V. Ortiz, B. B. Stefanov, G. Liu, A. Liashenko, P. Piskorz, I. Komaromi, R. Gomperts, R. L. Martin, D. J. Fox, T. Keith, M. A. Al-Laham, C. Y. Peng, A. Nanayakkara, C. Gonzalez, M. Challacombe, P. M. W. Gill, B. G. Johnson, W. Chen, M. W. Wong, J. L. Andres, M. Head-Gordon, E. S. Replogle, J. A. Pople, Gaussian, Inc., Pittsburgh PA, **1998**.

[11] M. J. Frisch, J. A. Polple, J. S. Binkley, *J. Chem. Phys.* **1984**, *80*, 3265−3269.

[12] A. D. Becke, *J. Chem. Phys.* **1993**, *98*, 5648−5652.

[13] M. W. Wong, K. B. Wiberg, M. J. Frisch, *J. Am. Chem. Soc.* **1992**, *114*, 1645.

[14] S. David, O. Eisenstein, W. J. Hehre, L. Salem, R. Hoffmann, *J. Am. Chem. Soc.* **1973**, *95*, 3806−3807.

Received May ö23, 2002
[O02273]